Photocathode studies for robust PICOSEC Micromegas detectors

CERN Summer Student Programme 2023 Report

Chiara Volpato
Supervisors: Marta Lisowska, Florian Brunbauer

Università degli Studi di Firenze, Florence, Italy
Master in Physical and Astrophysical Science

Abstract

Contemporary experiments in High Energy Physics (HEP) require precise timing detectors to ensure the accurate reconstruction of particle tracks and identification of the origin points (vertices) of these particles. The PICOSEC MicroMegas (MM) collaboration is working on the development of a precise timing detector based on the MicroMegas technology. The primary objective of this detector is to achieve exceptional timing precision, and it has already demonstrated promising results in the realm of tens of picoseconds.
At CERN, the Gaseous Detectors Development (GDD) team is working on multiple PICOSEC MM prototypes in view of developments to make it scalable for broader applications, refining its timing resolution, and enhancing its overall durability.
This report details the implementation of the single photoelectron measument and analysis, as well as the procedure used for testing different types of photocathodes, in pursuit of creating a more robust detector.

Keywords: MicroMegas, PICOSEC, Timing detectors, Cherenkov detectors, Photocathode

1. Introduction

In today's HEP experiments, energies and collision rates are increasing significantly. To effectively explore particles within such high-energy environments, detectors are required to have high time resolution to reduce the pile-up and enable accurate vertices reconstruction. The PICOSEC MM collaboration aims to develop a spatially scalable, stable and robust gaseous detector with timing resolution in the range of tens of picoseconds. They have developed some prototypes of the PICOSEC MM detector which are currently undergoing testing and analysis to further optimize timing resolution, detector stability and robustness. In particular, I have been involved in testing different photocathode materials to enhance robustness. To do this, I implemented the method for acquiring and analysing data in the configuration of single photoelectron measurement.

1.1. PICOSEC Detector Concept

The PICOSEC detector technology is based on the MicroMegas structure. As shown in Figure 1, a typical MicoMegas comprises a cathode, a mesh and an anode, with the space between the cathode and the anode filled with gas. When a charged particle passes through this volume, it ionises some gas molecules, freeing electrons. These electrons are guided by the electric field to the mesh (drift gap), where they are accelerated and start an avalanche (amplification gap). This type of detector is not suitable for precise timing measurements due to ionization occurring at various points within the detector, resulting in irreducible time jitter. To overcome this limitation, the PICOSEC detector incorporates a layer of Cherenkov radiator at the entrance (see Figure 2). In this configuration, when a charged particle traveling at sufficient speed to produce Cherenkov effect passes through the detector, it generates a cone of photons that then reach the photocathode coated on the surface of the radiator which converts the Cherenkov light to primary electrons. In this way, the multiplication starts always

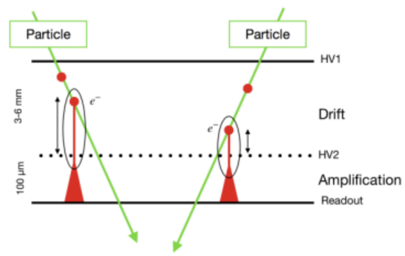

Figure 1: General structure of a MicroMegas detector. We can see the difference in timing for two different particles crossing the detector at the same moment.

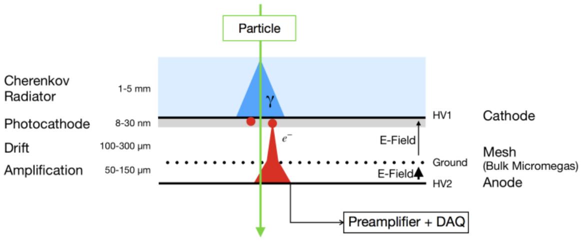

Figure 2: General structure of a PICOSEC detector.

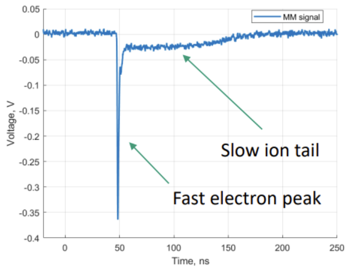

Figure 3: Typical PICOSEC signal.

at the same time and the same location, leading to improved time resolutions. The gas used in the PICOSEC detectors is $Ne/C_2H_6/CF_4$ (80/10/10). The standard crystal used is a 3 mm thick MgF_2, with a Cr layer for electrical connection, on top of which the photocathode is coated. The typical signal obtained is illustrated in Figure 3, featuring a fast electron peak and a slower ion tail.

Ongoing development efforts for practical PICOSEC detectors are focused on several aspects, including achieving robustness, scalability, and granularity. For this reason, the detector has been built in different dimensions, as shown in Picture 4: single pad detector, multi pad and 10x10 module.

Research is also underway to enhance the preamplification gap for uniformity and thinness, to refine electronics with the creation of dedicated amplifiers and multi-channel digitalizers, and to improve photocathode materials for increased durability.

1.2. Motivation for photocathodes studies

The photocathode material that was first used for the PICOSEC detector is the Cesium Iodine (CsI), which has high quantum efficiency with respect to other materials (approximately one order of magnitude more) and produces high number of photoelectrons. However, CsI gets damaged by ion

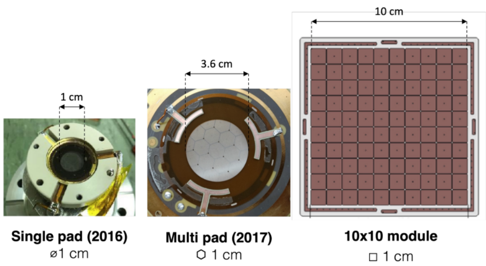

Figure 4: Different sizes of the PICOSEC detector.

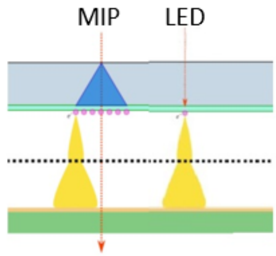

Figure 5: Different interactions of a MIP and of LED photons in the configurations of single photoelectron produced.

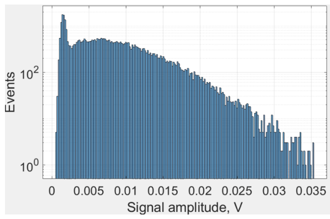

Figure 6: Distribution of the maximums of each waveform amplitude with LED source in the configuration of single photoelectron produced.

backflow and discharges, and it is highly sensitive to humidity. These characteristics make CsI photocathodes challenging to handle during assembly and they tend to degrade rapidly.

These issues prompted the need to explore alternative photocathode materials that are more robust, such as Diamond Like Carbon (DLC) and Boron Carbide (B_4C).

To compare the performance of different photocathodes, the Number of PhotoElctrons (NPE) generated during the amplification process is used. This number can be estimated as the ratio between the signal amplitude when a Minimum Ionising Particle (MIP) crosses the detector and the amplitude when the avalanche is started by a single photoelectron (see Figure 5).

To extract the NPE, two different measurements for each photocathode are conducted. At first an LED is used as light source ensuring operation in single photoelectron configuration. The waveforms are recorded and for each the maximum amplitude is selected and reported in a histogram (as depicted in Fig. 6). Subsequently, the histogram is fit to extract the mean maximum signal amplitude. The same procedure is repeated using MIPs as source. With these data, the NPE produced can be calculated as:

$$\mathrm{NPE} = \frac{\text{MIP fit mean}}{\text{SPE fit mean}}. \tag{1}$$

To perform these studies the single pad detector is used, changing different photocathodes (one example is in Pictures 7).

2. Transparency measurements

The NPE produced after the amplification with a specific photocathode can be influenced by different factors, such as

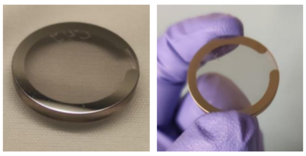

Figure 7: Two samples of B_4C deposited on the 3 mm MgF_2 crystal with the Cr ring visible.

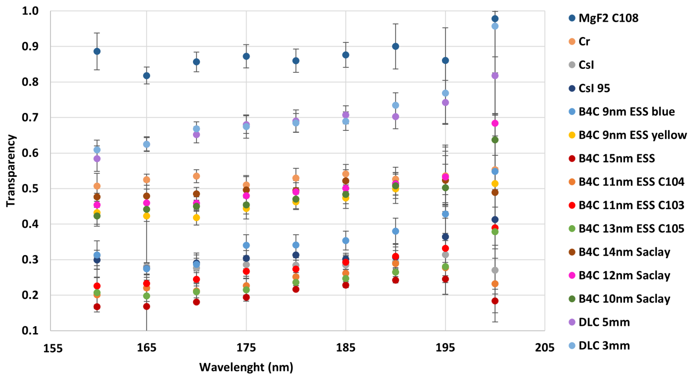

Figure 8: Transparency measuments for the different photocathodes at different wavelenghts of the incident light.

the material and the thickness. Since different samples are produced by different collaborators, ESS and Saclay, and with different techniques, it's possible that the nominal thickness does not accurately reflect the actual thickness. To be able to compare different photocathodes, transparency measurements were performed: the sample is irradiated with UV light of known intensity, and the wavelenght is scanned using a monochromator. It is then measured how much of the light passes through the photocatode. By calculating the ratio between the beam's intensity with and without the sample, we obtained the transparency of the photocathode. Different photocathodes were tested: multiple samples of B_4C from Saclay and from ESS, some samples of CsI, of DLC, a layer of MgF_2 crystal and one with only the Cr deposition. The results obtained are displayed in chart 8.

As expected, the layer of MgF_2 without any deposition has the highest transparency. Following we have the two samples of DLC, which do not have the Cr layer on top. Next there is the MgF_2 crystal with the deposition of Cr. For the B_4C photocathodes, all the thicknesses produced from Saclay are close together at almost the same transparency, and the same for the ones from ESS, with only three samples deviating from this trend. The two 9 nm thick: the "yellow", being the thinest, and the "blue" being thicker, and the thickest of 15 nm, having as expected the lowest transparency measured.

This measurements are now useful for comparing different photocathodes based on their transparency rather than on the nominal thickness.

3. Robust photocathode studies

3.1. New procedure of acquiring and analyzing data

To determine the NPE produced after the amplification, the signal waveforms are acquired using a charge sensitive preamplifier (the signal obtained is shown in Figure 9). Fore each waveform the highest amplitude point is selected, a histogram is filled with these maximum signal amplitudes and the distribution obtained is fit with a Polya function. The focus is the average value given by the distribution fit.

It can be seen from the example 10 that in doing so there were some problematic fits, likely due to the fact that the distinction between noise events and signal events is not always clear-cut, with the overlapping of noise peak and signal peak causing the impossibility of having an accurate fit.

To address this issue, a new data acquisition and analysis method was conceived to enhance clarity in distinguishing noise from signal. To achieve a clear distinction between noise and signal, the first thing to do is to acquire a dataset of signal and noise events with the LED switched on. Next, maintaining the same trigger threshold, is to acquire a dataset of noise events only, with the LED switched off. At this point the analysis processes before the 'only noise' dataset, filling a histogram with the maximum waveform amplitudes and fitting it with a Gaussian distribution. The mean and sigma values obtained from this fit are passed to the analysis of the 'noise+signal' dataset: it fills a histogram with the maximum value of each waveform and it fits the distribution with a Gaussian+Polya distribution. The starting parameters for the Gaussian portion of the distribution are derived from the earlier 'only noise' fit. As shown in the example 11, this method successfully improves the way of fitting the maximum amplitude distributions of the single photoelectron analysis. Consequently, this procedure now allows to extract accurately the average maximum amplitude in the case of signals generated by a single photoelectron (LED source).

Regarding the signals produced by a MIP, we acquire data from a muon beam triggering on an external tracker (as detailed in section 3.3). For this reason we do not have a noise peak and so there is no need of this newly implemented procedure, but we can fit the histogram using only a Polya distribution (Figure

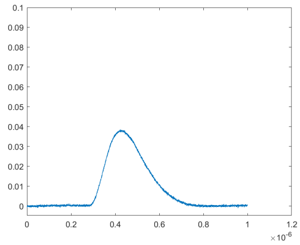

Figure 9: Typical PICOSEC signal using a charge sensitive preamplifier.

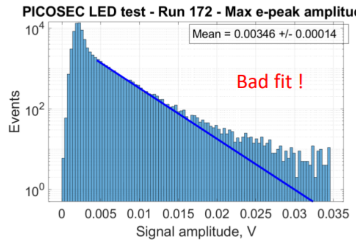

Figure 10: Example of problematic fit from April 2023 RD51 test beam.

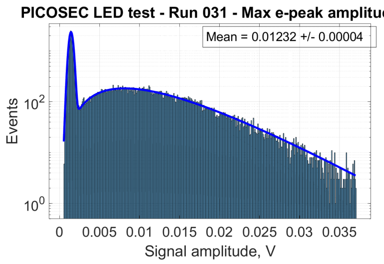

Figure 11: Typical fit of the maximum signal amplitudes distribution with the implemented procedure of acquiring and measuring in the case of LED source (example from August 2023 test beam).

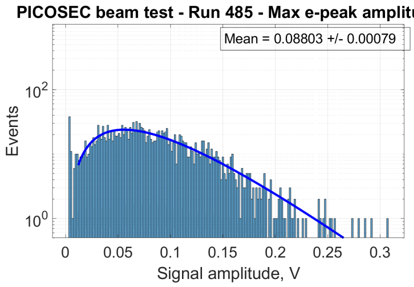

Figure 12: Typical fit of the maximum signal amplitudes distribution in the case of muon beam.

12).
From these two different fits we obtain the two mean values of the signals that enable us to calculate the number of photoelectrons produced after the amplification.

3.2. *Laboratory measurements*

Since in the laboratory it is possible to measure only using the LED as light source, Single Photoelectron (SPE) measurements were carried out in order to train the code, test the new procedure and test new photocathodes before using them in the test beam.
The detector was composed of a MgF_2 Cherenkov radiator 3 mm thick and 1 inch of diameter, photocathode of B_4C plus Cr layer, preamplification gap of 150 µm and amplification gap of 128 µm. It was placed in a hermetic vessel (Figure 13) working in sealed mode at a constant preassure of 990 mbar. The measurements were acquired keeping the anode voltage constant at 275 V and varying the cathode voltage (540 V, 550 V, 560 V). The photocathodes tested are three different B4C thicknesses

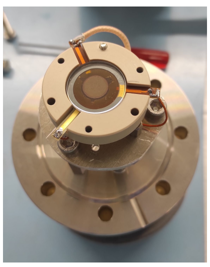

Figure 13: Detector prototype assembled in hermetic vessel used for SPE measurements in the lab.

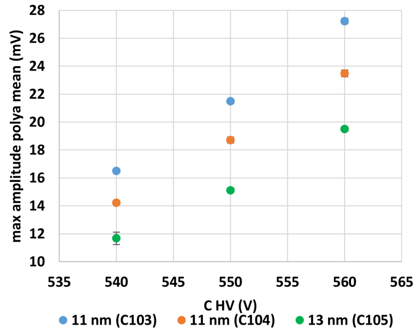

Figure 14: Results of the averages of the maximum amplitudes given from the fit for the 3 photocathodes in function of the cathode voltage applied.

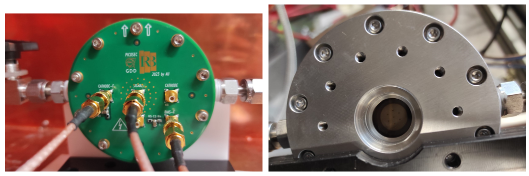

(a) (b)

Figure 15: Chamber used for SPE measurements in the lab and in August test beam: board 15(a) and window 15(b).

from ESS, identified as follows:
- C103 (nominal thickness 11 nm)
- C104 (nominal thickness 11 nm)
- C105 (nominal thickness 13 nm).

The results obtained are presented in the graph 14. The error bars shown in this plot, as always in this report regarding this type of fit, only represent the component from the fits, which underestimates the total errors. Other contributions depend on the oscilloscope scale, on the trigger level, on the number of events per bin (acquisition time, LED rate, histogram binning).
Looking at the trend it can be seen that, as expected, the amplitude increases with the voltage. Simultaneously, the amplitudes should remain consistent for different photocathodes under the same conditions (same detector, pressure, voltages). This is expected because, when working in the condition of single photoelectron, the type or thickness of the photocathode should not influence the amplitude of the signal but rather the event rate. However, it can be clearly seen that these amplitudes are different.
To better understand this unexpected variation, additional measurements were conducted using a different chamber and a different detector. In this case, the chamber is the one in the Pictures 15, and the preamplification gap is 130 µm, thinner that with the hermetic chamber. The results obtained are presented in graph 16, revealing that the observed trend between the photocathodes remains the same despite the change in detector.

3.3. *Test beam measurements*

Studies with MIPs as source were conducted during two test beam: one in July and another in August 2023, during which different types of photocathodes were tested. In a test beam

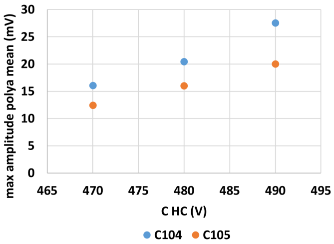

Figure 16: Results of the averages of the maximum amplitudes given from the fit for 2 of the 3 photocathodes in function of the cathode voltage applied.

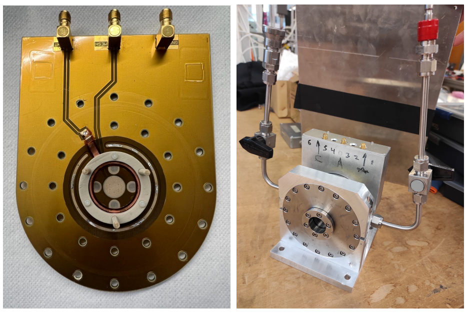

(a) (b)

Figure 17: Chamber used for beam measurements in July.

campaign, the opportunity arises to perform measurements both in single photoelectron configuration (using an LED source) and with a muon beam. Combining these two sets of measurements yields the NPE produced after the amplification for each photocathode.

In the first campaign the measurements were conducted with the chamber in Figure 17, which has the same characteristics of the other chambers used except for the preamplification gap, set at 145 µm. The anode voltage was kept constant at 275 V and the cathode voltage varied from 470 V to 530 V. The detector operated in flushing mode, which meant that temperature fluctuations throughout the day caused pressure changes. To address this issue, the signal amplitude loss over time was examined using the chamber depicted in Figure 15. Since a 3% loss in one day has been observed, this chamber was used in sealed mode for the August test beam, as data acquisition sessions during the test last for several hours. The anode voltage was kept constant at 275 V and the cathode voltage was varied from 470 V to 490 V (except for CsI which ranged from 410 V to 430 V).

In both cases, the chambers are placed in a telescope (Figure 18) capable of tracking with GEMs, triggering and time reference with MCP-PMTs, and timing with MMs. When acquiring data with the muon beam, the trigger is set on an external detector, one of the MPC, to exclude noise events. Furthermore, only tracks with the Cherenkov cone fully contained within the detector are selected, meaning within a circular area of 2 mm in radius for the 3 mm radiator.

The results obtained for the NPE produced are displayed in the charts 19 for the B_4C and DLC photocathodes. For CsI, which is the reference photocathode, in both cases NPE~20 PE. Notably, the anomalous values observed in July for the B_4C sample of 13 nm (C105) were not reproduced in a repeated measurement in August, aligning with the trend of the other samples. Additionally, the sample of B_4C 11 nm (C103) is used to say that the measurements in the two periods are consistent. Since no clear trend in NPE with respect to nominal thickness is evident, the results are plotted also as a function of measured transparency, as shown in graph 20. The NPE values displayed are the weighted means of the NPE at the different voltages, with errors propagated from the fits on the amplitude distributions. The errors associated with transparency values are provided by the measurement system. A better trend is observed and this correlates thinner photocathodes (with higher transparency) with increased NPE.

For the photocathodes analyzed in August test beam the means of the maximum signal amplitudes of SPE measurements at the same voltages for different photocathodes were compared, expecting them to be consistent since they were conducted under

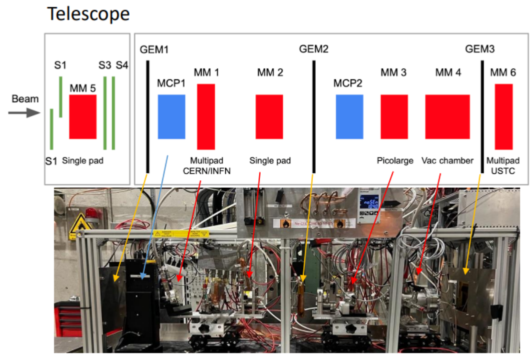

Figure 18: Telescope used in the July 2023 test beam campaign.

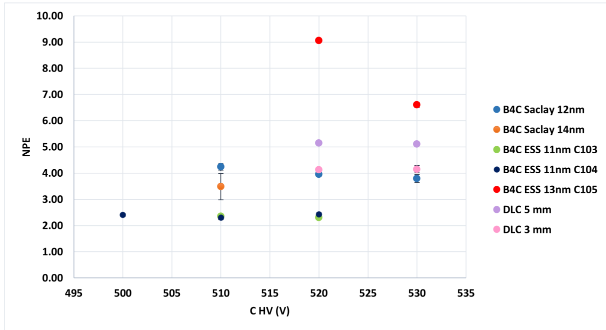

(a)

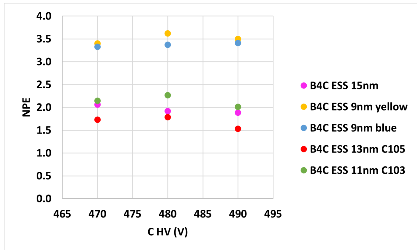

(b)

Figure 19: 19(a) NPE for the photocathodes tested in July and 19(b) in August.

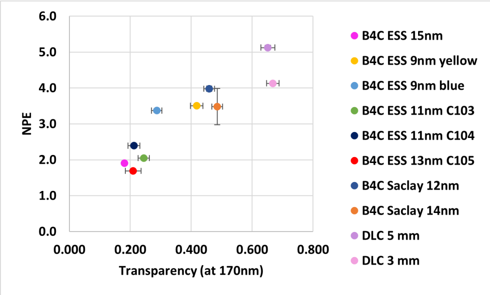

Figure 20: NPE Vs measured transparency at 170 nm.

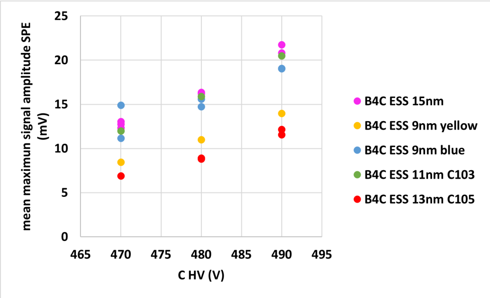

Figure 21: Means of the maximum signal amplitudes for SPE for the different photocathodes tested in August test beam.

the same conditions. This comparison is illustrated in Figure 21, but it can be observed that the values are not the same.

In each of these discrepancies, it must be acknowledged that the error on the mean maximum amplitude is underestimated, as it is based solely on the value provided by the fit. Other factors may also contribute to the observed variations.

4. Conclusions

During these three months at CERN, I tested various types of robust photocathode materials of different thicknesses and from different producers for applications in a precise timing detector. My work contibutes to the search for new materials that can offer sufficiently good performances to replace the CsI photocathode. While CsI provides great quantum efficiency and timing resolution in PICOSEC MM detectors, it gets damaged very easily by humidity and ion back flow.

We do not yet have a material that produces as many PE as the CsI, but we are reaching quite high NPE with DLC and we are on the way for understanding how the NPE is related to the photocathode thickness, having higher NPE for thinner photocathodes.

I also played a role in this research by implementing the way of acquiring and analizing data in the configuration of single photoelectron production, introducing a new procedure which yielded satisfactory results, particularly regarding the new fit applied to the distribution of maximum signal amplitudes.

5. Acknowledgments

During my time in the GDD lab, I had the privilege of working on various aspects of research. I spent several sessions in the cleanroom, where I worked with different types of chambers, changed photocathodes and assembled some 10x10 module detectors. I also gained experience in using the ASSET for the transparency measurements. Moreover, I had the opportunity to participate in two separate two-week-long test beam, where I was involved in assembling the telescopes, collecting and analyzing data. These experiences allowed me to learn valuable skills, such as working effectively in a professional laboratory setting, planning experiments to achieve specific objectives, and coordinating efforts towards a common goal.

I would like to express my gratitude to Marta, my supervisor at CERN, for providing me with this incredible opportunity and for her guidance and support throughout my time here. I also want to extend my thanks to the entire GDD group, especially Florian Brunbauer and Eraldo Oliveri, as well as all the collaborating groups during the beam tests. Working with you all was truly enhancing.

I would also like to acknowledge the support and guidance of Lorenzo Bonechi and Vitaliano Ciulli, my professors in Florence, who supported me and helped me throughout my academic journey. In particular, I am grateful for their assistance in making it possible for me to spend these months at CERN.

References

- T. Tabarelli-de-Fatis, A timing layer in CMS for the High-Luminosity LHC (2018)
- L. Sohl, Development of PICOSEC-Micromegas for fast timing in high rate environments (2021)
- M. Lisowska, NDIP (2022)
- M. Lisowska, MPGD2022